AJNR

Fast spin-echo imaging in the evaluation of intradural disease of the spine.

G Sze, M Merriam, K Oshio and F A Jolesz

AJNR Am J Neuroradiol 1992, 13 (5) 1383-1392
http://www.ajnr.org/content/13/5/1383

Fast Spin-Echo Imaging in the Evaluation of Intradural Disease of the Spine

Gordon Sze,[1,3] Michael Merriam,[1] Koichi Oshio,[2] and Ferenc A. Jolesz[2]

PURPOSE: Fast spin echo (FSE) images were compared with conventional images in 46 patients with intradural spinal disease to determine their accuracy in the detection and delineation of lesions. **MATERIALS AND METHODS:** The images were interpreted by two neuroradiologists, who read individually. A total of 720 blinded readings formed the basis for this evaluation. A gold standard for each patient was selected, based on the blinded readings of the conventional studies. **RESULTS:** In the sagittal plane, the FSE sequences were found to have an accuracy of 93% and 93% for the first reader and 93% and 85% for the second reader. For the axial plane, the corresponding figures were 86% and 82% for the first reader and 64% and 77% for the second reader. These figures compared favorably with conventional sequences. Similar delineation of lesions was noted in 78% of cases. In the remaining cases, there were no significant trends. **CONCLUSION:** Because of these findings, FSE sequences appear as accurate as conventional sequences. In this study, they were capable of supplanting conventional sequences in the evaluation of intradural pathology of the spine in the sagittal plane, although conventional sequences were still preferred in the axial plane.

Index terms: Spinal cord, magnetic resonance; Magnetic resonance, technique

AJNR 13:1383–1392, Sep/Oct 1992

The fast spin echo (FSE) sequences, variants of the original RARE (rapid acquisition with relaxation enhancement) sequence (1–4), may potentially replace long repetition time (TR) spin-echo (SE) imaging in the evaluation of the brain and spine (5, 6). Before routine use of this new sequence can be accepted, however, careful evaluation must demonstrate that the FSE sequences can truly replicate the quality and sensitivity of conventional sequences in a shorter amount of time. This study was performed to compare FSE sequences with routine long TR cardiac-gated SE sequences and, where appropriate, with gradient echo (GRE) sequences in the evaluation of intradural pathology.

Received September 19, 1991; revision requested November 12, received January 6, 1992, and accepted on January 27.

[1] Department of Radiology, Yale University School of Medicine, New Haven, CT.

[2] Department of Radiology, Brigham and Women's Hospital, Boston, MA.

[3] Address reprint requests to Gordon Sze, MD, Yale University School of Medicine, Department of Radiology, 333 Cedar Street, New Haven, CT 06510.

AJNR 13:1383–1392, Sep/Oct 1992 0195-6108/92/1305-1383

Materials and Methods

Forty-six patients with lesions of the cord or intradural extramedullary space demonstrated by conventional long TR SE imaging were evaluated with FSE sequences. In the sagittal plane, long TR SE acquisitions were performed with cardiac gating in the cervical and thoracic spine and with gradient moment nulling in the first order in the frequency-encoding and section select directions in all cases. Echo times (TE) were 30 to 35 msec for the first echo and 70 to 80 msec for the second echo. TR ranged from 1800 to 2600 msec in the cervical and thoracic spine. One excitation was used. The matrix was 256 × 192. Imaging times ranged from 9 min 12 sec to 19 min 20 sec. TR ranged from 1600 to 2000 msec in the lumbar spine. One or two excitations were used. The matrix was 256 × 192 or 256 × 256. Imaging times ranged from 6 min 48 sec to 12 min 30 sec. In 28 studies, imaging times fell between 10 and 15 min. In 11 studies, imaging times were greater than 15 min. Three-millimeter sections were obtained in all cases.

In the axial plane, three-dimensional Fourier transform (3DFT) GRE images were performed in the cervical spine, utilizing parameters of 50/15/5 (TR/TE/flip angle) and gradient moment nulling in the frequency-encoding direction. Two excitations were used. The matrix was 256 × 192. Imaging time was 9 min 38 sec. Twenty-eight 3-mm sections were obtained after the two end sections on either

side were discarded. In the thoracolumbar and lumbar spine, where less cerebrospinal fluid (CSF) pulsation was present, long TR SE sequences were used in six cases. The parameters were 1600–2000/30,80. One or two excitations were used. The matrix was 256 × 192. Gradient moment nulling in the frequency-encoding and section select directions was used. Imaging times ranged from 6 min 48 sec to 10 min 35 sec. Section thickness ranged from 3–5 mm, depending on the nature of the pathology.

The FSE sequences used in this study have been previously described (6, 7) and were performed with parameters optimized for the MR evaluation of the cord. In the sagittal plane, patients were studied with TR of 2000 to 3000 msec with effective TE of 18-42 msec and 88-126 msec. Two excitations were used. The echo train consisted for 8 echoes and the echo spacing was 14–18 msec. Imaging times varied from 3 min 12 sec to 4 min 1 sec. Three-millimeter sections were obtained in all cases.

In 22 patients, axial scans were also performed, using either a 3DFT FSE multislab technique in the cervical and thoracic spine or a two-dimensional Fourier transform (2DFT) FSE sequence with identical parameters as in the sagittal plane in the lumbar spine. In the 3DFT multislab FSE technique, four slabs were excited with each slab phase encoded into eight sections in the section-slab direction (7). The parameters were 4000/90–112. One excitation was used. The echo train consisted of 12 echoes. The echo spacing was 14–18 msec. The matrix was 256 × 192. Time of acquisition was 8 min 36 sec. Twenty-four 3-mm contiguous sections were obtained in all cases after the end section of each slab was discarded.

The images from all of the 46 patients were separated into five sets, consisting of FSE sagittal, FSE axial, SE sagittal, SE axial, and GRE axial. Scans from 21 normal patients were also intermixed with the study scans. One set of images from each patient was randomly selected and displayed on an alternator. Two neuroradiologists, each by himself and blinded to clinical history, read the scans. Information regarding the type of pulse sequence performed was obscured. The readers could not be totally blinded to whether the study was FSE or SE because this differentiation can sometimes be seen on the images themselves due to the increased signal of lipid on the long TR/long TE FSE or due to mild blurring on the long TR/short TE FSE (Fig. 1). Often, however, when parameters were optimized and, because of the high intensity of lipid adjacent to the surface coil even on routine long TR SE images, definitive judgment on the type of acquisition was difficult.

Each reading of one set of images was separated from readings of other sets of images from the same patient by at least a week to decrease the likelihood of readers remembering the results of a previous set of images. Each set of images was read two separate times by each reader. The typical patient, then, had either eight or 16 blinded readings, depending on whether or not axial scans were performed, four each of the FSE sagittal, FSE axial, SE sagittal, and SE axial or GRE axial. A total of 720 blinded interpretations were performed, 544 of which were of the 46 patients with abnormalities.

The readers evaluated the images for sensitivity in the detection and delineation of pathology. With respect to sensitivity, a standardized questionnaire was used for each set of images. The presence or absence of a lesion was indicated by selecting the appropriate response from 1 to 5, with 1 = images definitely normal, 2 = images probably normal, 3 = images possibly normal, 4 = images probably abnormal, and 5 = images definitely abnormal. Other ancillary information, such as the number of lesions, any associated cord swelling, the presence or absence of any magnetic susceptibility artifacts that might be indicative of the nature of the lesion, such as hemosiderin, and the differential diagnosis, was also requested.

After the blinded readings were completed, a "gold standard" was established for each patient, against which the FSE sequences were compared. Each set of the conventional images, that is, the SE sagittals and SE or GRE axials, had four separate blinded readings, two from each reader. If the readings on at least three of the four scans were concordant, this reading was accepted as the gold standard. In cases of discrepancy, the entire conventional study, consisting of all long TR SE and/or GRE sequences, was reviewed, and a final reading was established.

Each blinded reading was graded as positive or negative depending upon whether or not lesions were detected. A positive reading was defined as a score of 4 or 5. A negative reading was classified as a score of 1 to 3. The accuracy of each sequence in correctly detecting pathology was computed for the 46 patients by calculating the percentage of correct responses for any given blinded reading. An analysis of variance (ANOVA) was performed on the readers' responses. The inter-reader and intra-reader reliability were calculated using Spearman's correlation for ranks.

With respect to the ability of FSE sequences to delineate the size and shape of lesions, a schematic diagram of spine and cord was included in the blinded evaluations so that lesions could be directly indicated pictorially on the questionnaire. In this way, the accuracy of estimates of lesion size and configuration could be assessed. The lesions were also measured in size with a pair of calipers. The length and width of each lesion were recorded at their longest dimensions in the sagittal images. Separate measurements were made for the FSE and SE scans. If the difference in one dimension fell within 25% of the larger measurement, the lesions were felt to be of equal size on both sequences. If the difference in one dimension differed by greater than 25% of the larger measurement, the lesions were felt to be of different sizes on the two sequences.

Results

Table 1 lists the suspected pathologies. Surgical pathology was available in 14 cases. In the remainder, the diagnosis was based on the results of the gold standard findings combined with the results of other sequences, such as contrast-enhanced short TR sequences, and with the clinical history. In 29 cases, the lesion involved the

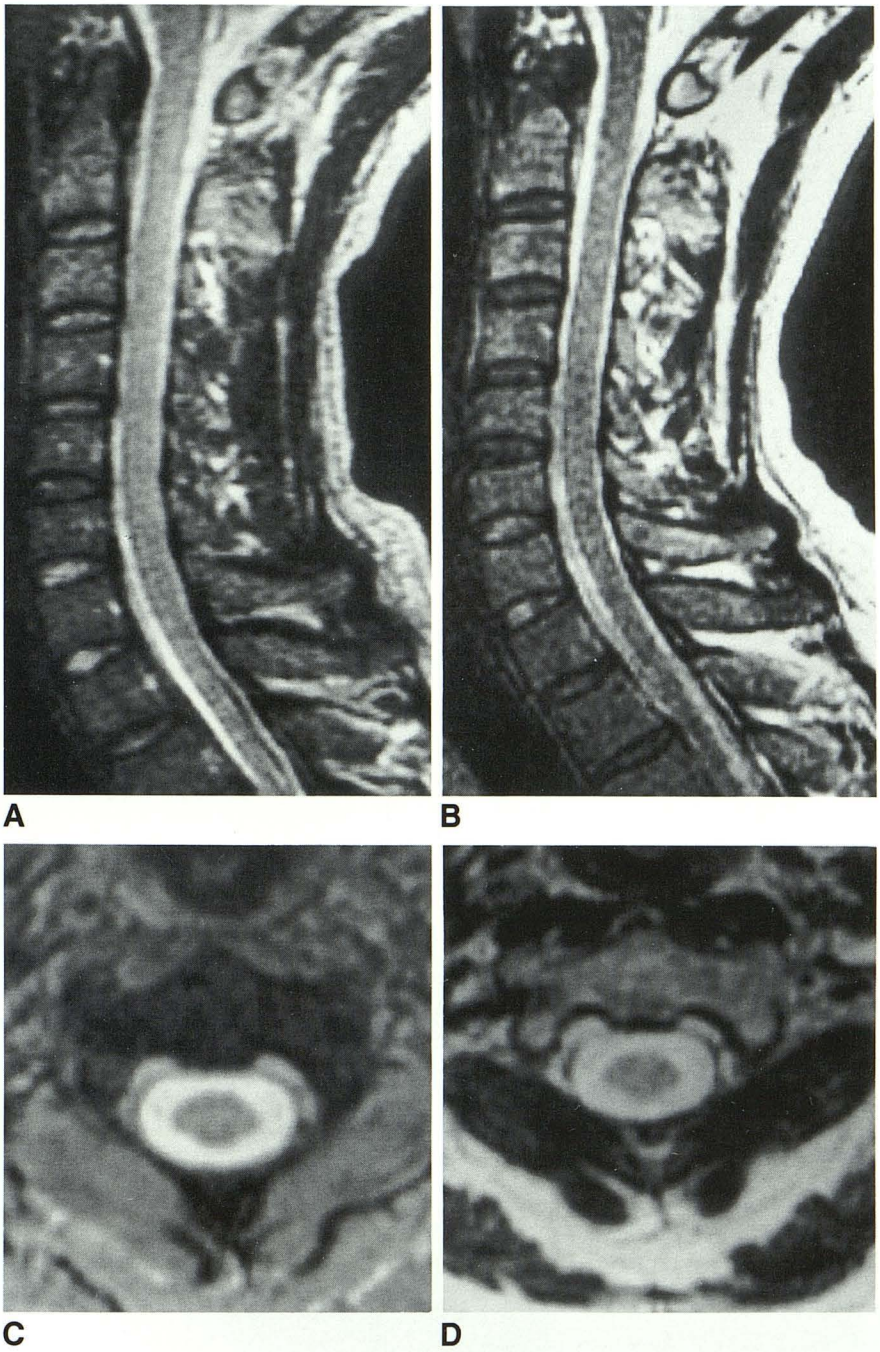

Fig. 1. Normal sagittal and axial SE and FSE images of the cervical spine.

A, Cardiac-gated long TR (1905/80) sagittal SE image with gradient moment nulling. The time of acquisition was 12 min 33 sec.

B, Long TR (2000/126), echo train length 8, echo spacing 14 msec, sagittal FSE image. Note greater signal intensity of subcutaneous and marrow fat. The time of acquisition was 3 min 12 sec.

C, 3DFT GRE (500/15/5) axial image. The time of acquisition was 9 min 38 sec.

D, 3DFT FSE (4000/112), echo train length 12, echo spacing 14 msec, axial image. Note the greater signal intensity of fat and the decreased gray-white matter differentiation. The time of acquisition was 8 min 36 sec.

TABLE 1: Intradural pathology of the patients

Multiple sclerosis	21
Syrinx	6
Glioma of the cord	5
Ischemia/gliosis	4
Infectious myelitis	3
Vascular malformation	3
Neuroma/neurofibroma	1
Meningioma	1
Arachnoiditis	1
Changes from surgical rhizotomy	1

cervical region. In 20 cases, the thoracic region was affected. In nine cases, the lumbar region was involved. In 12 cases, the lesion extended over more than one area of the spine.

In the sagittal plane, of the 46 cases, 43 (93%) were considered positive in the FSE sequences by the first reader in the first blinded reading and 43 (93%) in the second (Figs. 2–4). For the second reader, the corresponding figures were 43 (93%) and 39 (85%). Forty-one (89%) cases were found to be positive in the SE sequences by the

Fig. 2. Fifty-nine-year-old woman with multiple sclerosis and symptoms of myelopathy.

A, Long TR (1935/30,80) cardiac-gated sagittal SE image shows a plaque in the cord at the level of C2. The time of acquisition was 12 min 30 sec.

B, Long TR (2000/35,88), echo train length 8, echo spacing 18 msec, sagittal FSE image also demonstrates the plaque well. The time of acquisition was 3 min 13 sec.

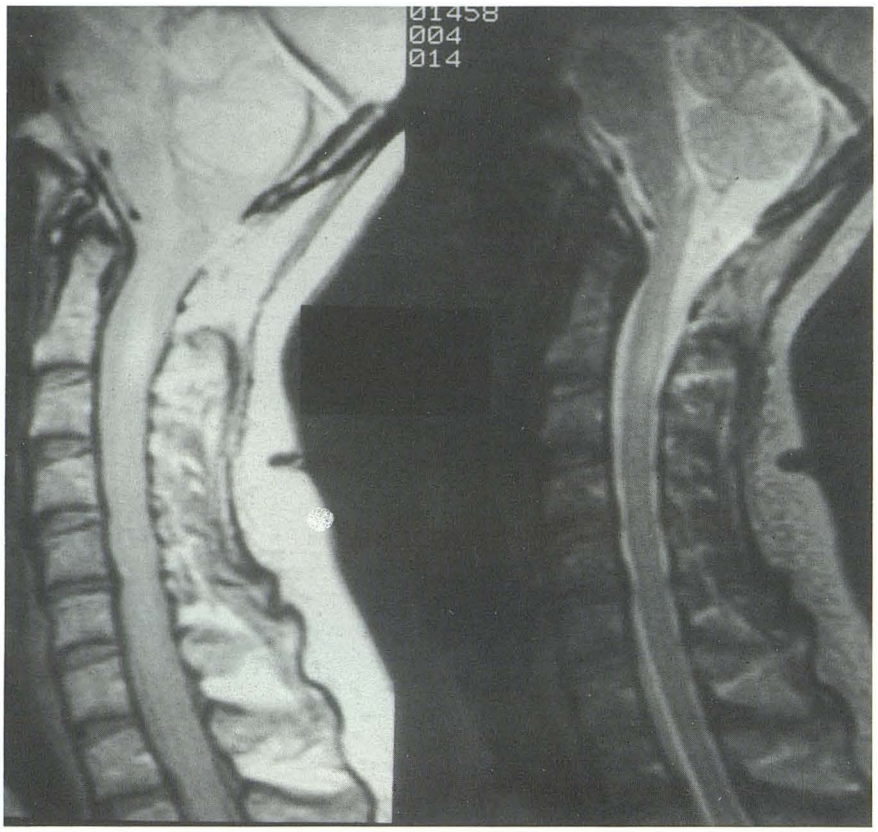

A

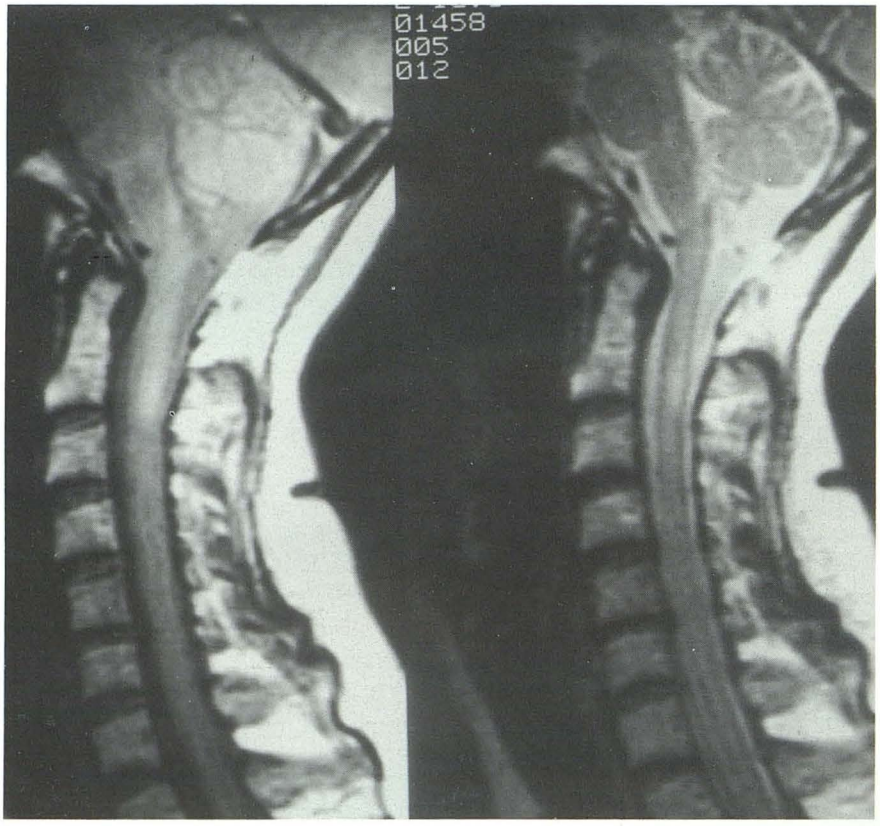

B

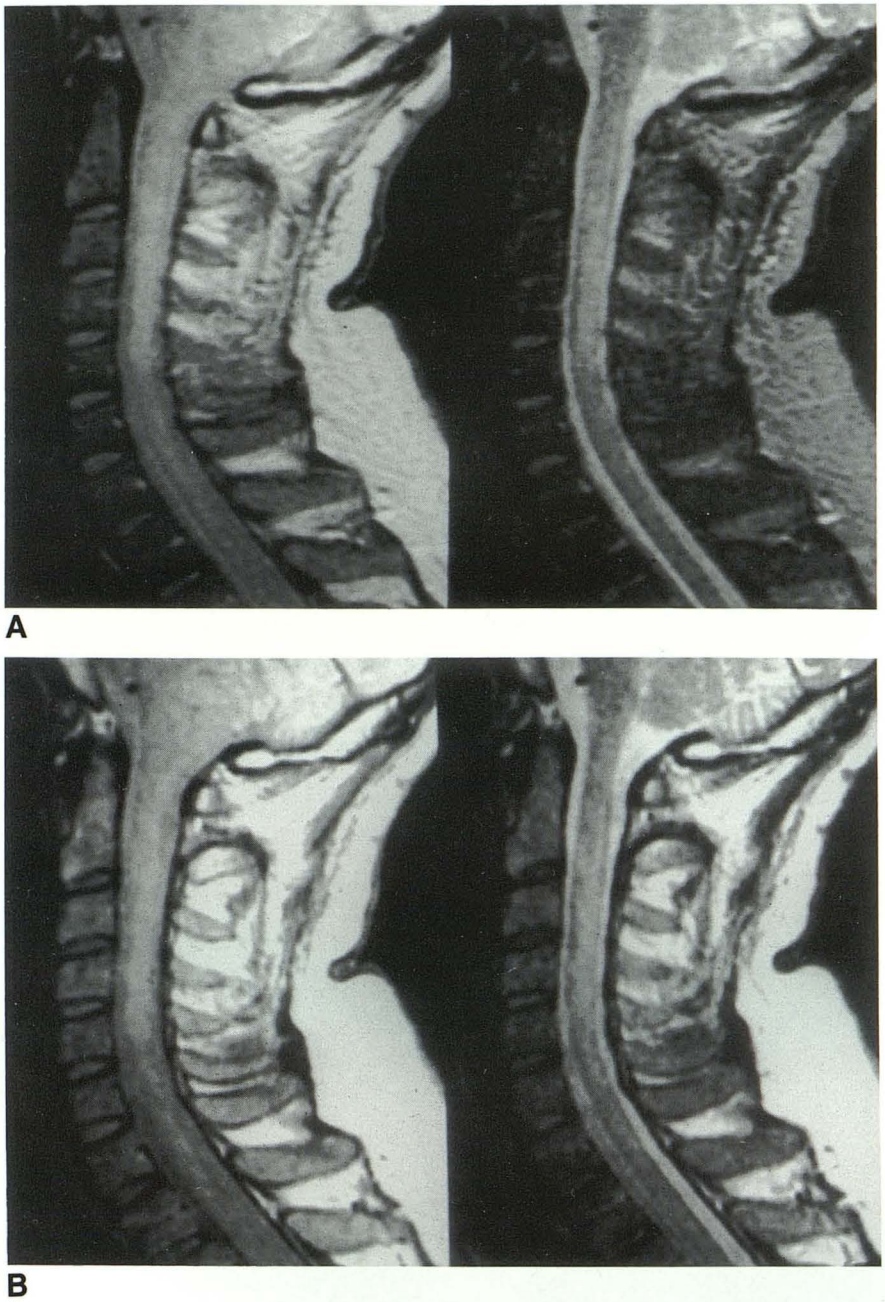

Fig. 3. Forty-two-year-old man with multiple sclerosis.

A, Cardiac-gated long TR (2449/30,80) sagittal SE image demonstrates poorly defined high signal intensity in the upper cervical cord. The time of acquisition was 16 min 34 sec.

B, Long TR (2000/35,88), echo train length 8, echo spacing 14 msec, sagittal FSE image discloses findings similar in both intensity and delineation. The time of acquisition was 3 min 17 sec.

first reader in the first blinded reading and 42 (91%) were positive to the second reading. For the second reader, the corresponding figures were 37 (80%) and 44 (96%). In the axial plane, of the 22 cases, 19 (86%) were positive in the FSE by the first reader in the first blinded reading and 18 (82%) in the second (Fig. 5). The corresponding figures were 14 (64%) and 17 (77%) for the second reader. Twenty-one (95%) cases were interpreted as positive in the conventional sequences by the first reader in the first blinded reading and 19 (86%) in the second. For the second reader, the corresponding figures were 15 (68%) and 18 (82%).

An ANOVA on the readers' responses revealed no significant differences between reader performance using SE or FSE for either the sagittal or axial planes (Fig. 6). For normal scans in the sagittal plane, the means of 1.463 and 1.275, for SE and FSE, were not found to be significantly different, $F(1,38) = 1.75$, $P = .194$. For abnormal scans in the sagittal plane the means of 4.511 and 4.592, for SE and FSE, were not found to be significantly different, $F(1,90) < 1.00$. For abnor-

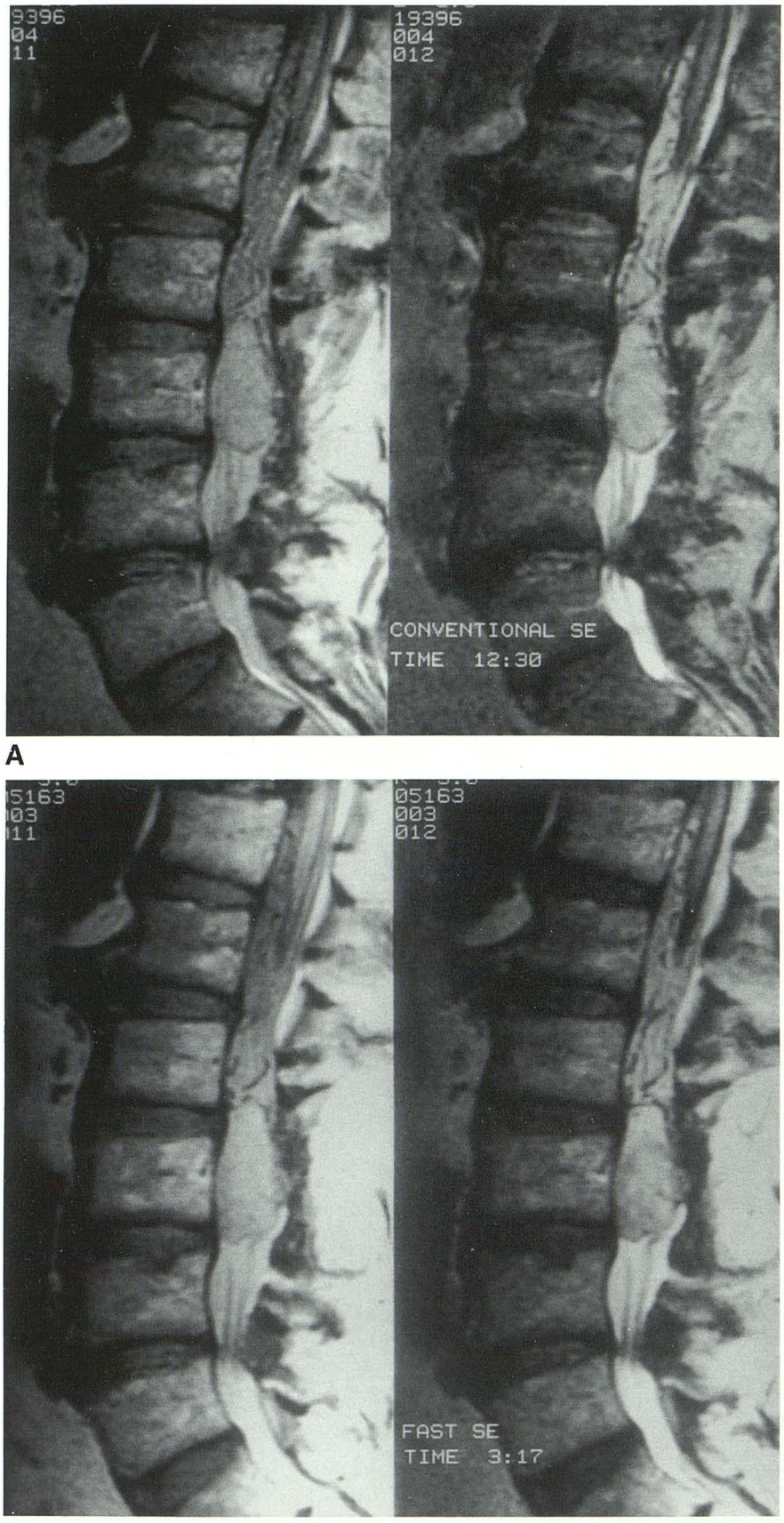

Fig. 4. Seventy-nine-year-old man with ependymoma.

A, Long TR (1600/30,80) sagittal SE image depicts a mass centered posterior to the L3 vertebra with distorted nerve roots superiorly. Also seen is mild hypointensity outlining the conus and nerve roots, consistent with hemosiderin deposition from previous tumor bleeds. The time of acquisition was 12 min 30 sec.

B, Long TR (2000/35,88), echo train length 8, echo spacing 18 msec, sagittal FSE image confirms the presence of the mass. Although hypointensity due to hemosiderin deposition is not as well seen on the first TE, it is clearly demonstrated on the second TE. The time of acquisition was 3 min 17 sec.

A

B

Fig. 5. Thirty-five-year-old woman with a well-documented history of multiple sclerosis, presenting with paresthesias of the right arm and leg.

A, Axial GRE images (50/15/5) shows the presence of a large plaque, involving much of the central gray matter and peripheral white matter on the right side of the cord. Its location was consistent with the patient's symptomatology. The time of acquisition was 9 min 38 sec.

B, 3DFT FSE (4000/112), echo train length 12, echo spacing 14 msec, image demonstrates the plaque in a similar location as on the axial GRE. The time of acquisition was 8 min 36 sec.

mal scans in the axial plane, the means of 4.440 and 4.193, for SE and FSE, were not found to be significantly different, $F(1,41) < 1.00$.

Both the intra-reader and inter-reader reliabilities were calculated using Spearman's correlation for ranks. All reliabilities were quite high and indicated consistent performance within and across readers. The intra-reader reliabilities were $r = .836$, $P = .0001$, and $r = .846$, $P = .0001$ for readers one and two, respectively, while the inter-reader reliability was $r = .783$, $P = .0001$.

With respect to the delineation of lesions, on the SE sequences, no lesions were less than 5 mm in length, eight were 5–10 mm, and five were 10–20 mm. The remainder were larger than 20 mm in length. Twenty-two lesions were less than 5 mm in width and 14 were 5–10 mm. The lesions were measured to be similar in size on FSE and SE sequences in 36 of the 46 (78%) cases. In the remaining 10, the lesions differed in size of the FSE images as opposed to the SE images. When these 10 cases were reviewed, however, an underlying reason, such as movement between sequences or a poorly defined border to the lesion, was found. No significant trend was seen. In three cases, the FSE measurement was larger, while in seven cases, the SE measurement was larger.

Discussion

In this study, the choice of which conventional sequences to perform in the protocol was based on what was interpreted as standard practice. For example, long TR SE sequences are generally considered the most sensitive acquisitions in the sagittal plane, although some authors contend that GRE sequences may be equally, but not more, sensitive (8, 9). Similarly, 3DFT GRE sequences are usually felt to be optimal for evaluation of suspected lesions of the cervical cord in the axial plane (8, 9). Our aim, therefore, was to compare the optimized conventional study against the FSE study.

The generic FSE sequences in this study consisted of a 90° excitation pulse followed by an echo train of variable length, usually 4, 8, 12, or 16 echoes (6, 7). The interecho spacing could be varied, although it is often kept between 14-20 msec. Each echo was separately phase-encoded and phase was rewound after each echo. The TE corresponded to that echo at which the phase encodes with the smallest amplitudes were applied. Data collected with these "low-order" phase encode gradients controlled image contrast. In the dual echo sequences employed in this study, the first four echoes were used in the formation of the spin-density image and the later four echoes contributed to the heavily T2-weighted image.

A number of potential disadvantages were seen with FSE imaging. First, for a given TR, a smaller number of sections could be obtained with the 2DFT FSE sequences than with the SE sequences. For the purposes of spine imaging, however, only a limited number of sections is required and the decreased number of sections for a given TR did not prove to be a significant problem in this study. Second, a theoretical loss

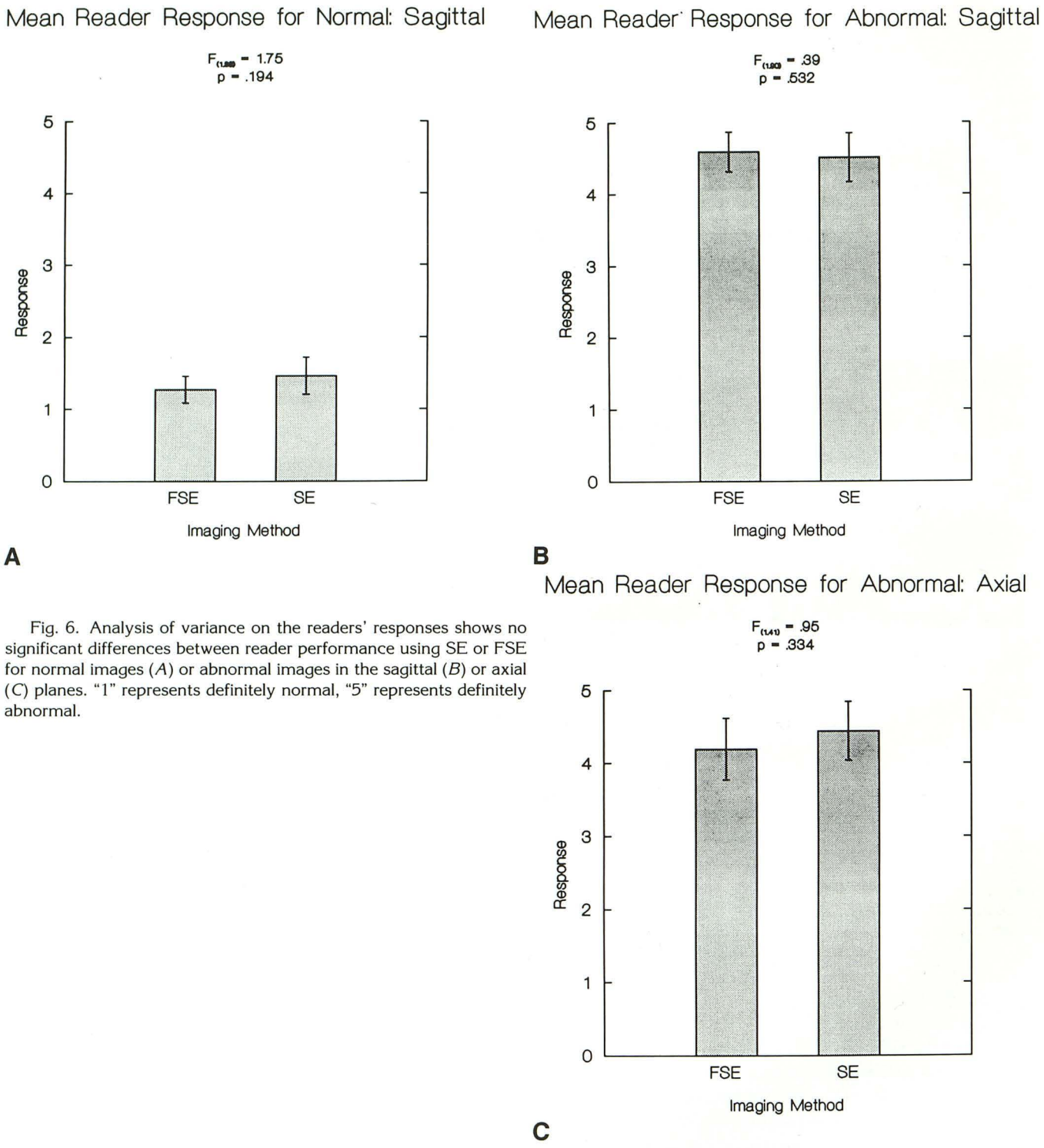

Fig. 6. Analysis of variance on the readers' responses shows no significant differences between reader performance using SE or FSE for normal images (*A*) or abnormal images in the sagittal (*B*) or axial (*C*) planes. "1" represents definitely normal, "5" represents definitely abnormal.

of small object contrast has been proposed in FSE imaging, using computer simulations of lesions two pixels in size (10). The loss of small object contrast was found to be more prominent with substances that had a short T2 relaxation time and on spin-density sequences. Possibly because our lesions had long T2 relaxation times and possibly because the lesions in the study, although small, were all larger than two pixels, no difference in accuracy was noted between FSE and SE imaging. Third, conventional methods of compensating for CSF pulsation, that is, cardiac gating and gradient moment nulling, were either time consuming (cardiac gating) or difficult to implement due to the short interecho spacing (gradient moment nulling). Because of this, the

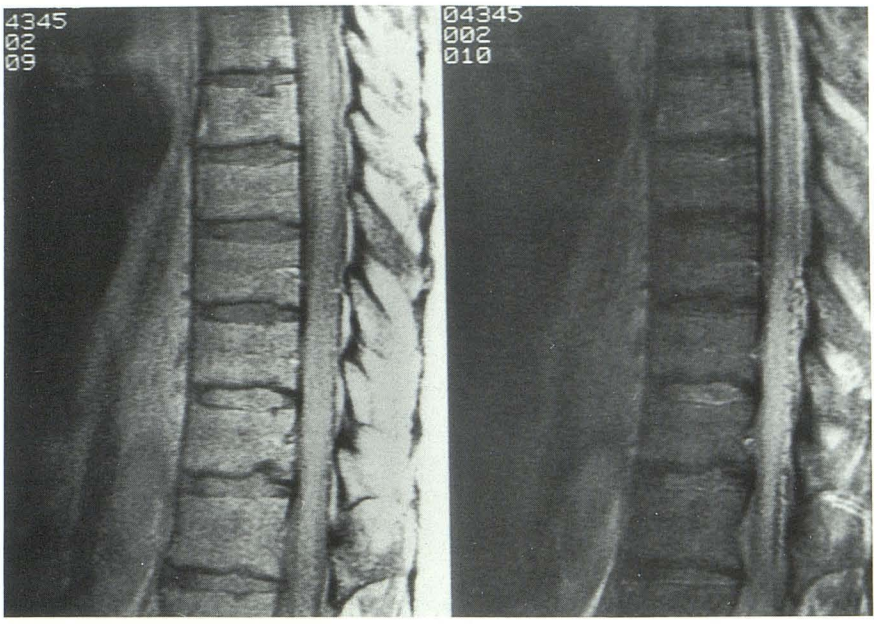

A

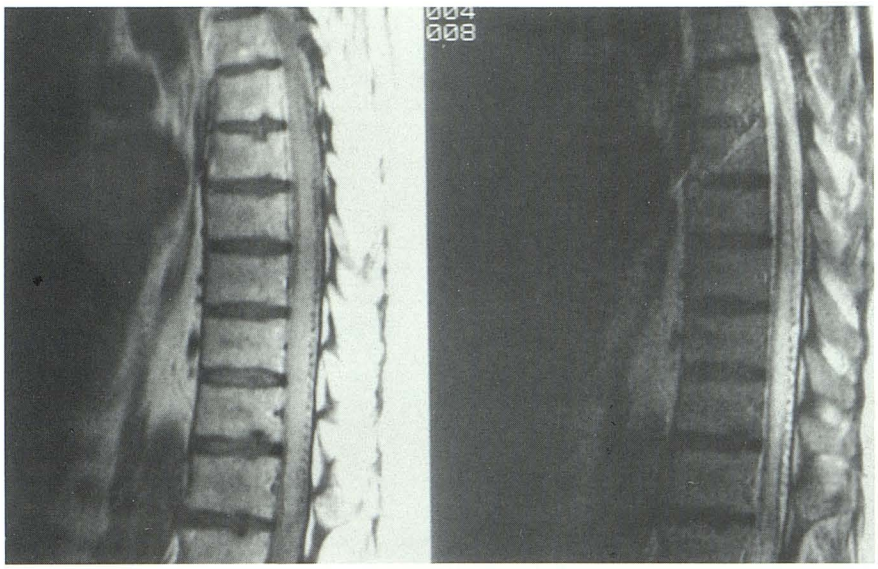

B

Fig. 7. Sixty-five-year-old man with myelopathy. Pathology: dural arteriovenous fistula.

A, Cardiac-gated long TR (1690/30,80) sagittal image shows high signal intensity in the cord associated with punctate foci of high signal and signal void posterior to the cord. Time of acquisition was 14 min 29 sec.

B, Long TR (2500/18,126), echo train length 8, echo spacing 14 msec, sagittal FSE image exhibits similar findings. The punctate signal voids are even better detected on the spin-density FSE than the spin-density SE study, possibly due to the influence of gradient moment nulling in the latter. Time of acquisition was 2 min 46 sec.

CSF signal in some of the images in this study was not always as homogeneous or as high in intensity as in the SE images when similar parameters were employed. Since the decreased intensity of CSF signal in the FSE images did not appear to affect the ability to detect lesions in the cord, it was not felt to be a significant deficit in this study. To produce homogeneous high signal CSF, it was necessary to vary parameters, for example, by increasing the TE, optimizing echo train length and echo spacing, and interchanging phase- and frequency-encoding axes. At the conclusion of the study, gradient moment nulling became available, permitting the acquisition of images with parameters similar to those in SE imaging that had more homogeneous and high signal intensity in the CSF.

As previously noted, the FSE sequences in this study were distinguished by persistence of signal of lipid in the subcutaneous tissue and in the vertebral body marrow in the long TR/long TE FSE images compared with the long TR/long TE SE images (Fig. 1) (6). This difference may be due to a coupling interaction between different protons induced by the very short echo spacing (6). Otherwise, contrast in the FSE images appeared strikingly similar to that of the SE images.

Contrast in the 3DFT FSE axial images differed from that of the 3DFT GRE axial images. Although gray-white contrast has been noted to be

increased in 2DFT FSE images in the brain compared to SE images, due to magnetization transfer effects (11), gray-white contrast in the cord was markedly decreased compared to the GRE images (Fig. 1). This decrease did not appear to affect the accuracy of interpretation according to analysis of the blinded readings but was felt to provide less optimal images by both readers.

The decreased magnetic susceptibility effects of FSE were also noted in this study (Fig. 4). Magnetic susceptibility effects of hemosiderin are due to diffusion-related dephasing induced by the field gradients generated by the paramagnetic iron-containing molecules and were thus decreased in the FSE sequences because of the short interecho spacing (6). This decreased magnetic susceptibility did not prove to obscure visualization of products of hemorrhage when heavily T2-weighted FSE images were examined (Fig. 4) and proved beneficial in cases in which large osteophytes or changes associated with previous surgery were present.

Narrowing of the vascular structures has been noted in FSE images of the head (6). Conceivably, this difference could result in decreased visualization of arteriovenous malformations or dural arteriovenous fistulas in the spine. In both cases, however, short TR SE sequences are generally the procedure of choice for the detection of the small signal voids of flowing vessels since gradient moment nulling techniques sometimes obscure visualization on conventional long TR SE or GRE acquisitions. In cases in this study, signal void of flowing vessels in dural vascular malformations was equally well seen on the FSE sequences as on the long TR SE sequences (Fig. 7).

In conclusion, the FSE images of 46 patients with intradural spinal lesions were compared to the conventional images and were found to be of equal sensitivity in the detection and delineation of pathology. With the exception of 3DFT FSE axial acquisitions, FSE sequences were generally much more rapid than conventional studies of the spine, especially long TR cardiac-gated SE sequences. FSE sequences were considered to be capable of replacing conventional sequences in the evaluation of suspected intradural spinal lesions in the sagittal plane; in the axial plane, however, 3DFT GRE sequences were still felt to be superior due to better gray-white matter differentiation in the cord.

Acknowledgment

The authors thank Allen Ashworth, PhD, of the Yale Statistics Consulting Service for performance of the statistical analysis.

References

1. Hennig J, Naureth A, Friedburg H. RARE imaging: a fast imaging method for clinical MR. *Magn Reson Med* 1986;3:823–833
2. Hennig J, Friedburg H, Strobel B. Rapid nontomographic approach to MR myelography without contrast agents. *J Comput Assist Tomogr* 1986;10:375–378
3. Hennig J, Friedburg H, Ott D. Fast three-dimensional imaging of cerebrospinal fluid. *Magn Reson Med* 1987;5:380–383
4. Hennig J, Friedburg H. Clinical applications and methodological developments of the RARE technique. *Magn Reson Imaging* 1988;6: 391–395
5. Mulkern RV, Wong STS, Winalski C, Jolesz FA. Contrast manipulation and artifact assessment of 2D and 3D RARE sequences. *Magn Reson Imaging* 1990;8:557–566
6. Melki PS, Mulkern RV, Panych LP, Jolesz FA. Comparing the FAISE method with conventional dual-echo sequences. *J Magn Reson Imaging* 1991;1:319–326
7. Oshio K, Jolesz FA, Milki PS, Mulkern RV. T2-weighted thin slice imaging with multi-slab 3D RARE. *JMRI* 1991;1:695–700
8. Katz BH, Quencer RM, Hinks RS. Comparison of gradient-recalled-echo and T2-weighted spin-echo pulse sequences in intramedullary s spinal lesions. *AJNR* 1989;10:815–822
9. Enzmann DR, Rubin JB. Cervical spine: MR imaging with a partial flip angle, gradient-refocused pulse sequence. II. Spinal cord disease. *Radiology* 1988;166:473–478
10. Constable RT, Gore JC. The loss of small objects in variable TE imaging: implications for FASE, RARE, and EPI. *Magn Reson Med* (in press)
11. Melki PS, Mulkern RV. Magnetization transfer effects in multi-slice RARE sequences. *Magn Reson Med* (in press)